Fungal Genetics and Biology 172 (2024) 103894

Contents lists available at ScienceDirect

Fungal Genetics and Biology

journal homepage: www.elsevier.com/locate/yfgbi

Regular Articles

The pleiotropic phenotype of FlbA of *Aspergillus niger* is explained in part by the activity of seven of its downstream-regulated transcription factors

Xiaoyi Chen [a], Juan P. Moran Torres [a], Peter Jan Vonk [a], J. Mirjam A. Damen [b], Karli R. Reiding [b], Jan Dijksterhuis [c], Luis G. Lugones [a], Han A.B. Wösten [a,*]

[a] *Microbiology, Department of Biology, Utrecht University, Padualaan 8, 3584 CH Utrecht, The Netherlands*
[b] *Biomolecular Mass Spectrometry and Proteomics, Bijvoet Center for Biomolecular Research and Utrecht Institute for Pharmaceutical Sciences, Utrecht University, Padualaan 8, 3584 CH Utrecht, The Netherlands*
[c] *Westerdijk Fungal Biodiversity Institute, Uppsalalaan 8, 3584 CT Utrecht, The Netherlands*

ARTICLE INFO

Keywords:
Fungus
Aspergillus
FlbA
Asexual development
Secretion
Cell wall stress

ABSTRACT

Inactivation of *flbA* in *Aspergillus niger* results in thinner cell walls, increased cell lysis, abolished sporulation, and an increased secretome complexity. A total of 36 transcription factor (TF) genes are differentially expressed in Δ*flbA*. Here, seven of these genes (*abaA*, *aslA*, *aslB*, *azf1, htfA*, *nosA*, and *srbA*) were inactivated. Inactivation of each of these genes affected sporulation and, with the exception of *abaA,* cell wall integrity and protein secretion. The impact on secretion was strongest in the case of Δ*aslA* and Δ*aslB* that showed increased pepsin, cellulase, and amylase activity. Biomass was reduced of agar cultures of Δ*abaA,* Δ*aslA*, Δ*nosA,* and Δ*srbA*, while biomass was higher in liquid shaken cultures of Δ*aslA* and Δ*aslB*. The Δ*aslA* and Δ*htfA* strains showed increased resistance to H_2O_2, while Δ*aslB* was more sensitive to this reactive oxygen species. Together, inactivation of the seven TF genes impacted biomass formation, sporulation, protein secretion, and stress resistance, and thereby these genes explain at least part of the pleiotropic phenotype of Δ*flbA* of *A. niger*.

1. Introduction

Aspergillus species can grow on a wide variety of organic substrates and in a broad range of abiotic conditions (Krijgsheld et al., 2013a). This and the fact that aspergilli disperse high numbers of asexual spores, called conidia, explains why these fungi are widespread in nature. Aspergilli secrete a large variety and quantity of enzymes to degrade their organic substrates into breakdown products that can serve as nutrients. Their high secretion capacity is used by the industry for large scale protein production (Wösten, 2019).

Sporulation and protein secretion are linked in *A. niger* (Levin et al., 2007; Krijgsheld et al., 2013b; Wang et al., 2015). This is illustrated by the finding that inactivation of *flbA,* which encodes a RGS domain protein, results in abolished sporulation and an increased secretome complexity. For instance, *ΔflbA* secretes a higher number of cellulases (from 10 to 16) and xylanases (from 9 to 16) (Krijgsheld et al., 2013b). Deletion of *flbA* not only impacts secretion and sporulation but also results in thinner cell walls and an increased cell lysis incidence. Moreover, 36 predicted transcription factor (TF) genes (Krijgsheld and Wösten, 2013; Aerts, 2018) are differentially expressed in Δ*flbA*. These TF genes have been proposed to be involved in the pleiotropic phenotype of Δ*flbA*. Here we studied the function of seven of these genes, i.e. *abaA* (*ATCC64974_20070*), *aslA* (*ATCC64974_80420*), *aslB* (*ATCC64974_91750*), *azf1* (*ATCC64974_32700*), *htfA* (*ATCC64974_81740*), *nosA* (*ATCC64974_82110*), and *srbA* (*ATCC64974_74890*). Expression of *aslA*, *azf1*, and *nosA* is reduced in Δ*flbA,* while *abaA, aslB, htfA,* and *srbA* are upregulated in this strain (Krijgsheld and Wösten, 2013).

Gene *aslA* of *Aspergillus nidulans* is involved in sporulation (Kim et al., 2017), acts as a repressor of sterigmatocystin production (Kim et al., 2017), and attenuates K^+ stress-inducible expression of genes involved in vacuolar sequestration of K^+ ions and vacuolar biogenesis (Park et al., 2015). Gene *nosA* of *Aspergillus fumigatus* represses vegetative growth and is involved in conidia formation in the dark (Soukup et al., 2012), while its homologue in *A. nidulans* functions in sexual development (Vienken and Fischer, 2006). Azf1 is involved in the formation of the mycotoxin ochratoxin A in *A. niger* (Wei et al., 2023). Its homologue in *Trichoderma reesei* modulates the expression of cellulase genes

* Corresponding author.
E-mail addresses: x.chen@uu.nl (X. Chen), j.p.morantorres@uu.nl (J.P. Moran Torres), p.j.vonk@uu.nl (P. Jan Vonk), j.m.a.damen@uu.nl (J.M.A. Damen), k.r.reiding@uu.nl (K.R. Reiding), j.dijksterhuis@wi.knaw.nl (J. Dijksterhuis), l.g.lugones@uu.nl (L.G. Lugones), h.a.b.wosten@uu.nl (H.A.B. Wösten).

https://doi.org/10.1016/j.fgb.2024.103894
Received 3 March 2024; Received in revised form 3 April 2024; Accepted 22 April 2024
Available online 23 April 2024

Table 1
A. niger strains used in this study.

Strain	Genotype	Reference
MA234.1	Δ*akuB, ΔkusA::DR-amdS-DR*	Park et al., 2016
Δ*abaA*	Δ*abaA, ΔakuB, ΔkusA::DR-amdS-DR*	This study
Δ*aslA*	Δ*aslA, ΔakuB, ΔkusA::DR-amdS-DR*	This study
Δ*aslB*	Δ*aslB, ΔakuB, ΔkusA::DR-amdS-DR*	This study
Δ*htfA*	Δ*htfA, ΔakuB, ΔkusA::DR-amdS-DR*	This study
Δ*azf1*	Δ*azf1, ΔakuB, ΔkusA::DR-amdS-DR*	This study
Δ*nosA*	Δ*nosA, ΔakuB, ΔkusA::DR-amdS-DR*	This study
Δ*srbA*	Δ*srbA, ΔakuB, ΔkusA::DR-amdS-DR*	This study
Δ*abaA::abaA*$^+$	Δ*abaA, ΔakuB, ΔkusA::DR-amdS-DR, abaA*$^+$	This study
Δ*aslA::aslA*$^+$	Δ*aslA, ΔakuB, ΔkusA::DR-amdS-DR, aslA*$^+$	This study
Δ*aslB::aslB*$^+$	Δ*aslB ΔakuB, ΔkusA::DR-amdS-DR, aslB*$^+$	This study
Δ*htfA::htfA*$^+$	Δ*htfA, ΔakuB, ΔkusA::DR-amdS-DR, htfA*$^+$	This study
Δ*azf1::azf1*$^+$	Δ*azf1, ΔakuB, ΔkusA::DR-amdS-DR, azf1*$^+$	This study
Δ*nosA::nosA*$^+$	Δ*nosA, ΔakuB, ΔkusA::DR-amdS-DR, nosA*$^+$	This study
Δ*srbA::srbA*$^+$	Δ*srbA, ΔakuB, ΔkusA::DR-amdS-DR, srbA*$^+$	This study

(Antonieto et al., 2019), while Azf1 of *Saccharomyces cerevisiae* regulates genes involved in cell wall maintenance when this yeast is grown on non-fermentable medium (Slattery et al., 2006).

Gene *abaA* encodes a central regulator of conidiophore formation in *A. nidulans* (Boylan et al., 1987), while SrbA of *A. fumigatus* and *A. nidulans* are involved in adaptation to hypoxia (Chung et al., 2014, Shukla et al., 2017; Rajasenan et al., 2022). SrbA of *A. fumigatus* is also involved in azole resistance (Zhang et al., 2021) and virulence (Chung et al., 2014). Genes *aslB* and *htfA* have not yet been characterized in *Aspergillus*. The former gene is highly similar to *aslA* of *A. niger* (see below), while *htfA* is a homologue of *FgHTF1* of *Fusarium graminearum*. The latter gene encodes a homeobox TF that is involved in the formation of aerial hyphae and conidiophores and that also may be involved in oxidative stress tolerance and cell wall modification (Fan et al., 2020).

Here we show that inactivation of *abaA, aslA, aslB, azf1, htfA, nosA,* and *srbA* reduces asexual sporulation in *A. niger*. Moreover, protein secretion and cell wall integrity are affected in all cases with the exception of Δ*abaA*. Finally, inactivation of some of the genes results in reduced or increased biomass formation and/or oxidative stress resistance. Together, these seven genes are involved in the pleiotropic phenotype of *flbA*.

2. Materials and methods

2.1. Strains and culture conditions

Escherichia coli TOP10 was used for constructing plasmids. Static and liquid cultures of *A. niger* strains (Table 1) were inoculated with spores and grown at 30 °C. Spores were isolated from 3-day-old cultures that had been grown on potato dextrose agar (PDA). To this end, 10^6 spores had been spread on the PDA plates. The spores were harvested with 0.9 % NaCl using a cotton swab. Hyphae were removed from the spore suspension by filtering through a syringe with cotton and the conidia in the resulting suspension were counted using a hemocytometer.

For static cultures, 10^6 spores were point inoculated in 9 cm Petri-dishes on minimal medium (MM; 70.6 mM $NaNO_3$, 11 mM KH_2PO_4, 6.7 mM KCl, 2 mM $MgSO_4{\cdot}7H_2O$, and trace element solution [Vishniac and Santer, 1957]) with 1 % glucose and 1.5 % agar (MMA-G). Glucose was replaced with 1 % (w/v) pectin, sucrose, xylose, xylan, starch, maltose, or sorbitol to assess sporulation on these carbon sources. Phenotyping of strains was also done on PDA. Colonies were grown in between two perforated polycarbonate membranes (pores of 0.1 μm, diameter 76 mm; Profiltra, Almere, The Netherlands) (Wösten et al., 1991) for RNA isolation and biomass assessment of static cultures. The upper polycarbonate membrane was placed 24 h after inoculation.

Liquid shaken cultures (80 mL medium in a 250 mL Erlenmeyer) were inoculated with 5 10^6 spores and grown at 200 rotations per min. Cultures were pre-grown for 16 h in transformation medium (TM; MM with 0.5 % yeast extract and 0.2 % casamino acids) with 25 mM glucose as a carbon source (TM-G). Mycelium was washed with 0.9 % NaCl and transferred to 80 mL MM-X (MM with 25 mM xylose) for 4 h (RNA-sequencing and qPCR) or 24 h (SDS-PAGE, proteomics, and qPCR). Biomass of liquid shaking cultures was determined from mycelium that had grown for 24 h on MM-G and that had been dried at 60 °C. For degradation of processed cellulose, this substrate (60 g/L w/v) (Recell, recell.eu) was pre-incubated for 24 h at 60 °C. This was followed by adding 4.5 g/L cellulose, 2.5 g/L yeast extract, and 1.0 g/L casamino acids. This mixture (CM-C) (50 mL in a 250 mL Erlenmeyer) was inoculated with 10^6 spores and grown for five days.

2.2. Gene inactivation constructs

Three plasmids were constructed for inactivation of each of the genes *abaA*, *aslA*, *aslB, azf1*, *htfA, nosA,* and *srbA*. Two plasmids were constructed to express a sgRNA targeting the 5′ and the 3′ end of the coding sequence of the target gene, respectively, while one construct was made in which flanking sequences of this gene were cloned (Supplemental Fig. 1A). The 23 bp sgRNAs were selected using CHOPCHOP (https://chopchop.cbu.uib.no/) and cloned between the proline tRNA promoter (ptRNA-pro1) and terminator (tracrRNA::term) using *PacI* linearized pFC332 (Nodvig et al., 2015). To this end, the promoter was amplified from vector pTLL108.1 (van Leeuwe et al., 2019) using primer pairs 1/3 (sgRNA1) and 1/17 (sgRNA2) (*abaA*), 1/4 (sgRNA1) and 1/18 (sgRNA2) (*aslA*), 1/5 (sgRNA1) and 1/19 (sgRNA2) (*aslB*), 1/6 (sgRNA1) and 1/20 (sgRNA2) (*htfA*), 1/7 (sgRNA1) and 1/21 (sgRNA2) (*azf1*), 1/8 (sgRNA1) and 1/22 (sgRNA2) (*nosA*), and 1/9 (sgRNA1) and 1/23 (sgRNA2) (*srbA*) (Supplemental Table 1). The terminator was amplified from plasmid pTLL109.2 (van Leeuwe et al., 2019) using primer pairs 2/10 (sgRNA1) and 2/24 (sgRNA2) (*abaA*), 2/11 (sgRNA1) and 2/25 (sgRNA2) (*aslA*), 2/12 (sgRNA1) and 2/26 (sgRNA2) (*aslB*), 2/13 (sgRNA1) and 2/27 (sgRNA2) (*htfA*), 2/14 (sgRNA1) and 2/28 (sgRNA2) (*azf1*), 2/15 (sgRNA1) and 2/29 (sgRNA2) (*nosA*), and 2/16 (sgRNA1) and 2/30 (sgRNA2) (*srbA*) (Supplemental Table 1). The promoter, terminator and sgRNA sequences were assembled using NEBuilder (New England Biolabs, international.neb.com) resulting in plasmids pFC332-sgRNA1-*abaA*, pFC332-sgRNA2-*abaA*, pFC332-sgRNA1-*aslA*, pFC332-sgRNA2-*aslA*, pFC332-sgRNA1-*aslB*, pFC332-sgRNA2-*aslB*, pFC332-sgRNA1-*azf1*, pFC332-sgRNA2-*azf1*, pFC332-sgRNA1-*htfA*, pFC332-sgRNA2-*htfA*, pFC332-sgRNA1-*nosA*, pFC332-sgRNA2-*nosA*, pFC332-sgRNA1-*srbA* and pFC332-sgRNA2-*srbA*.

The upstream and downstream fragments of the target genes were amplified from genomic DNA using primer pairs 31/32 (upstream *abaA*), 33/34 (upstream *aslA*), 35/36 (upstream *aslB*), 37/38 (upstream *htfA*), 39/40 (upstream *azf1*), 41/42 (upstream *nosA*), 43/44 (upstream *srbA*), 45/46 (downstream *abaA*), 47/48 (downstream *aslA*), 49/50 (downstream *aslB*), 51/52 (downstream *htfA*), 53/54 (downstream *azf1*), 55/56(downstream *nosA*) and 57/58 (downstream *srbA*) (Supplemental Table 1). The up- and downstream sequences of each gene were introduced in pUC19 (primer pair 153/154) using NEBuilder, yielding plasmids pUC19-*abaA*, pUC19-*aslA*, pUC19-*aslB*, pUC19-*htfA*, pUC19-*azf1*, pUC19-*nosA*, and pUC19-*srbA* (Supplemental Fig. 1B).

2.3. Constructs for reintroduction of genes

Two plasmids were constructed for reintroduction of genes *abaA*, *aslA*, *aslB, azf1*, *htfA, nosA,* and *srbA* in the respective deletion strains. One construct was made to express a sgRNA targeting either the 3′ end of the promoter or the 5′ end of the terminator of the target gene, while one construct was made in which the coding sequence and its flanking sequences were cloned (Supplemental Fig. 2A). The 23 bp sgRNAs were selected using CHOPCHOP and cloned between the proline tRNA promoter (ptRNA-pro1) and terminator (tracrRNA::term) using *PacI* linearized pFC332 (Nodvig et al., 2015). To this end, the promoter was amplified from plasmid pTLL108.1 using primer pairs 1/87 (*abaA*), 1/88

(*aslA*), 1/89 (*aslB*), 1/90 (*htfA*), 1/91 (*azf1*), 1/92 (*nosA*), and 1/93 (*srbA*), while the terminator was amplified from pTLL109.2 using primer pairs 94/2 (*abaA*), 95/2 (*aslA*), 96/2 (*aslB*), 97/2 (*htfA*), 98/2 (*azf1*), 99/2 (*nosA*), and 100/2 (*srbA*). This resulted in plasmids pFC332-gRNA-*abaA*-com, pFC332-gRNA-*aslA*-com, pFC332-gRNA-*aslB*-com, pFC332-gRNA-*htfA*-com, pFC332-gRNA-*azf1*-com, pFC332-gRNA-*nosA*-com, and pFC332-gRNA-*srbA*-com (Supplemental Fig. 2A).

5′ and 3′ flanks as well as the coding sequences of *abaA*, *aslA, aslB, azf1, htfA, nosA,* and *srbA* were amplified from genomic DNA by PCR using primer pairs 31/59 (*abaA* 5′ flank), 46/60 (*abaA* 3′ flank), 33/61 (*aslA* 5′ flank), 48/62 (*aslA* 3′ flank), 35/63 (*aslB* 5′ flank), 50/64 (*aslB* 3′ flank), 37/65 (*htfA* 5′ flank), 52/66 (*htfA* 3′ flank), 39/67 (*azf1* 5′ flank), 54/68 (*azf1* 3′flank), 41/69 (*nosA* 5′ flank), 43/70 (*nosA* 3′flank), 39/71 (*srbA* 5′ flank), 41/72 (*srbA* 3′flank), 73/74 (coding sequence *abaA*), 75/76 (coding sequence *aslA*), 77/78 (coding sequence *aslB*), 79/80 (coding sequence *htfA*), 81/82 (coding sequence *azf1*), 83/84 (coding sequence *nosA*), and 85/86 (coding sequence *srbA*) (Supplemental Table 1). As a result, a synonymous change of the third codon (contained in the 5′ primer of the coding sequence) was introduced, thereby enabling us to discriminate the reference strain from a strain in which the deleted gene was reintroduced. The PCR fragments were cloned in vector pUC19 using NEBuilder cloning kit (New England Biolabs), generating constructs pUC19-*abaA*-com, pUC19-*aslA*-com, pUC19-*aslB*-com, pUC19-*htfA*-com, pUC19-*azf1*-com, pUC19-*nosA*-com, and pUC19-*srbA*-com (Supplemental Fig. 2B).

2.4. Transformation of A. niger

Transformation of *A. niger* was done as described by de Bekker et al. (2009). Mycelium of 16-h TM-G liquid shaken cultures was protoplasted. Gene deletion was performed by co-transforming the three plasmids for each gene (see above). Transformants were selected on MMA-S (MMA medium with 2 M sucrose) with 150 μg mL^{-1} hygromycin, purified twice on MMA-G with 150 μg mL^{-1} hygromycin, and transferred to PDA without antibiotic. After 2 days, the colonies were transferred to MMA-G with or without 150 μg mL^{-1} hygromycin to confirm that the two sgRNA constructs (containing a hygromycin resistance cassette) were lost in the transformants. Gene deletion was confirmed by PCR using primer pairs 101/102 (*abaA*), 103/104 (*aslA*), 105/106 (*aslB*), 107/108 (*htfA*), 109/110 (*azf1*), 111/112 (*nosA*), and 113/114 (*srbA*) (Supplemental Table 1). The resulting fragments were sequenced (Macrogen, https://www.macrogen-europe.com) (Supplemental Fig. 1C).

Hygromycin was also used to select strains in which a deleted gene was reintroduced. Reintroduction was confirmed by PCR using primer pairs 115/116 and 117/118 (*abaA*), 119/120 and 121/122 (*aslA*), 123/124 and 125/126 (*aslB*), 127/128 and 129/130 (*htfA*), 131/132 and 133/134 (*azf1*), 135/136 and 137/138 (*nosA*), 139/140 and 141/142 (*srbA*) (Supplemental Table 1). The two resulting PCR fragments for each of the strains were sequenced (Macrogen) (Supplemental Fig. 2C).

2.5. qPCR

Expression levels of *agsA, chsC, gfaA, aguA, lacA, bglA, eglA,* and *amyA* in the reference and the deletion strains was assessed by qPCR using *actin* A as a reference gene. Total RNA was isolated as described (Krijgsheld et al., 2013b) from biological duplicates of 3-day-old sandwiched colonies grown on MMA-G for determining the expression level of *agsA, chsC,* and *gfaA*. On the other hand, total RNA was isolated as described (Aerts et al., 2019) from biological duplicates of liquid shaken cultures (16 h TM-G + 4 h MM-X and 16 h TM-G + 24 h MM-X) for quantifying the expression level of *aguA, lacA, bglA, eglA,* and *amyA*. RNA was purified with the NucleoSpin RNA Kit (Macherey-Nagel, https://www.mn-net.com) and reverse transcribed using the QuantiTect Reverse Transcription Kit (Qiagen, https://www.qiagen.com). The cDNA (1 ng) was used as a template for SYBR Green qPCR (Thermo Fisher, https://www.thermofisher.com) using 200 nM of the primer pairs 143/144 (*agsA*) (efficiency 91.4 %), 145/146 (*chsC*) (efficiency 98.4 %), 147/148 (*gfaA*) (efficiency 102.5 %), 153/154 (*aguA*) (efficiency 95.7 %), 155/156 (*lacA*) (efficiency 97.8 %), 157/158 (*bglA*) (efficiency 99.6 %), 159/160 (*eglA*) (efficiency 94.6 %), 161/162 (*amyA*) (efficiency 92.9 %) and 149/150 (*actin* A) (efficiency 97.21 %) (Supplemental Table 1). The total reaction volume was 10 μL. Samples were run on a ViiATM 7 Real-Time PCR System (Applied Biosystems, https://www.thermofisher.com) and analyzed using the $2^{-\Delta\Delta Ct}$ method.

2.6. RNA-sequencing

Mycelium of liquid shaken cultures of *A. niger* strains MA234.1, Δ*aslA,* and Δ*aslB* was homogenized in a Tissue Lyzer II (Qiagen) under liquid nitrogen. Total RNA was isolated using TRIzol reagent (Invitrogen, https://www.thermofisher.com), purified using the RNeasy Plant Mini Kit (Qiagen), and quantified with the Qubit RNA Broad Range Assay Kit on a Qubit 3 fluorometer (Thermo Scientific, https://www.thermofisher.com). Sequencing of RNA was performed with Illumina NextSeq2000 on a P2 flowcell with 2 x 50 bp paired-end technology (Utrecht Sequencing Facility; useq.nl). Read mapping against the *A. niger* N402 genome was performed with Hisat version 2.1.0 (Kim et al., 2019). Differential expression was determined from the aligned reads with Cuffdiff version 2.2.1, a part of the Cufflinks package (Trapnell et al., 2012). The terms “differentially expressed” and “over-expressed” refer to differences in Fragments per kilobase of transcript per million mapped reads (FPKM), and denote a fold change ≥ 4 with a minimum read number of 10 FPKM in at least one of the conditions. GO enrichment analyses were performed using the hypergeometric function to model the probability density using the “phyper” function from the R package stats. For the hypergeometric test we considered the universe size, N, to be the total number of EC numbers in all pathways in the genome, m the number of successes in this universe and defined as the number of EC numbers in the corresponding pathway in the genome, and k and x the sample size and the number of successes in the sample (or considered gene subset), respectively. Enrichments with a p-value $<$ 0.05 were considered significant.

2.7. SDS-PAGE

Proteins were precipitated overnight in 80 % pre-cooled acetone at −20 °C, collected at 4 °C at 20,000 g for 2 min and dissolved in loading buffer (20 % glycerol, 4 % SDS, 100 mM Tris-HCl pH 6.8, 0.01 % bromophenol blue). Composition and running of the polyacrylamide gels was done as described (Lyu et al., 2023).

2.8. Proteomics

Protein bands were excised, reduced with DTT, alkylated with iodoacetamide and in-gel digested with trypsin (Shevchenko et al., 2006). Nanoflow liquid chromatography coupled to mass spectrometry was performed on an Orbitrap Exploris mass spectrometer (Thermo Scientific) connected to a UHPLC 3000 system (Thermo Scientific). Approximately 20 % of the reconstituted peptides were loaded on a 300 μm diameter PepMap™ Neo Trap Cartridge and separated at 40 °C on a 50 cm × 75 μm Poroshell EC-C18 analytical column (2.7 μm). Solvent A consisted of 0.1 % formic acid, solvent B of 0.1 % formic acid in 80 % acetonitrile. Trapping was performed for 1 min in 9 % solvent B. Peptides were separated by a 37 min gradient of 9–44 % buffer B followed by 44–55 % B in 5 min, then 55–99 % B in 1 min, and 99 % B for 5 min. MS data were obtained in data-dependent acquisition mode. The full scans were acquired in the m/z range of 350–1600 at a resolution of 60,000 ($m\ z^{-1}$ 400) with AGC target 3 10^6. The most intense precursor ions were automatically selected for HCD fragmentation performed at normalized collision energy (NCE) of 28 % after accumulation to a target value of 10^5. MS MS acquisition^{-1} was performed at a resolution of

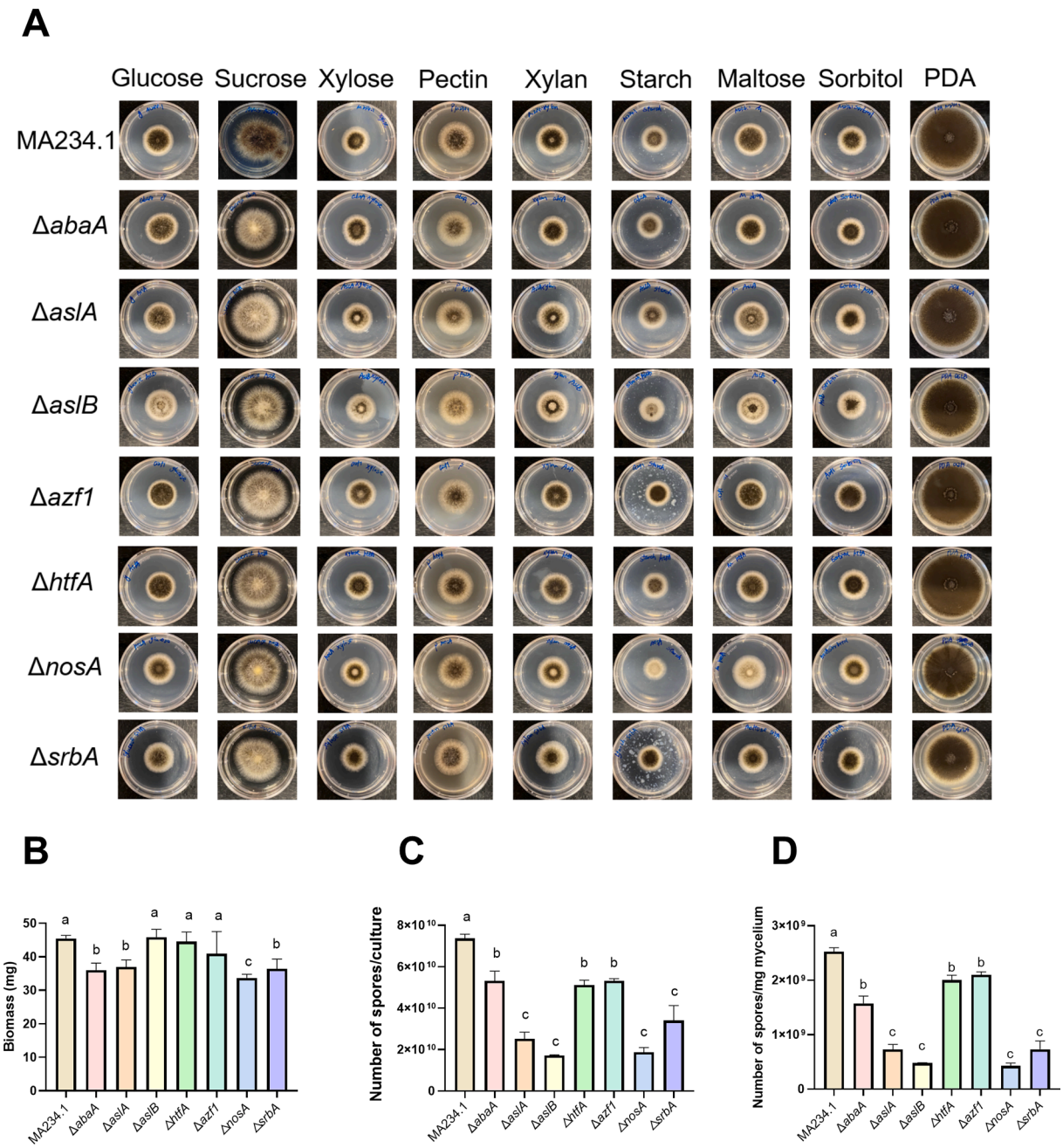

Fig. 1. Growth of *A. niger* strain MA234.1 and strains Δ*abaA*, Δ*aslA*, Δ*aslB*, Δ*azf1*, Δ*htfA*, Δ*nosA*, and Δ*srbA* on PDA and MMA with different carbon sources (A), as well as biomass (B), number of spores (C), and number of spores per mg mycelium (D) when grown on MMA-G. Cultures were grown for 5 (A) and 7 (B) days from a point inoculum or for 3 days after spreading of the spores on the agar medium (C, D). Statistical analysis was done with One-way ANOVA with different letters indicating statistical differences between strains.

15,000. For analysis of the MS data, peak lists were generated from the raw data files using the Proteome Discoverer software package version 3.0 (Thermo Scientific). Peptide identification was performed by searching the individual peak lists against a concatenated target-decoy database containing *A. niger* sequences in the SwissProt database, with the taxonomy set to other fungi, using the Mascot search engine (Matrix Science, https://www.matrixsciences.com) via the Proteome Discoverer interface. The search parameters included the use of trypsin as proteolytic enzyme allowing up to a maximum of 2 missed cleavages. Carbamidomethylation of cysteines was set as a fixed modification whereas oxidation of methionines was set as a variable modification. Precursor mass tolerance was set at 10 ppm, while fragment mass tolerance was set at 0.05 Da. Subsequently, the peptide identifications were filtered for an ion score of 20.

2.9. Enzyme activity assays

Cellulase activity was measured using the filter paper activity assay (Xiao et al., 2004). To this end, 7 mm diameter circles of Whatman No.1 filter paper were placed in wells of 96 well plates with 60 μLl culture medium for 24 h at 50 °C, followed by a 5 min incubation at 95 °C after adding 120 μL DNS (10 g/L 3,5-dinitrosalicylic acid, 400 g/L KNa-tartrate and 16 g/L NaOH). Samples (100 μL) were transferred to the 96 wells of a flat-bottom plate (Cellstar, Greiner Bio-one, https://www.gbo.com) and the A_{540} was determined using a Synergy HTX Microplate Reader (BioTek, https://www.agilent.com). Activity was determined

Table 2
Overview of the phenotypes of Δ*abaA*, Δ*aslA*, Δ*aslB*, Δ*azf1*, Δ*htfA*, Δ*nosA*, and Δ*srbA* when compared to the reference strain. Plate cultures were grown on glucose (MMA-G), while liquid shaken cultures were pre-grown on glucose (TM-G), after which growth was prolonged on the same carbon source (MM-X).

	Δ*abaA*	Δ*aslA*	Δ*aslB*	Δ*azf1*	Δ*htfA*	Δ*nosA*	Δ*srbA*
Plate cultures							
Conidia formation	down	down	down	down	down	down	down
Biomass glucose plates	down	down				down	down
SDS cell wall stress resistance	up	down	down	down	down	down	down
CR cell wall stress resistance	up					up	up
Resistance to H_2O_2		up	down		up		
Liquid shaken cultures							
Biomass liquid shaken cultures		up	up				
pH liquid shaken cultures		down	down		down	down	up

using a glucose standard curve. A unit of cellulase activity was defined as the release of 1 μmol glucose min^{-1}. Amylase activity was determined in a similar way as cellulase activity but the Whatman filter paper was replaced by 60 μl 1 % starch.

Xylanase activity was determined using the Xylanase Assay Kit (XylX6 Method) (Megazyme, https://www.megazyme.com). One unit of activity is the amount of enzyme required to release 1 μmol 4-nitrophenol min^{-1} from the XylX6 substrate under the defined assay conditions.

β-glucosidase activity was determined using the β-Glucosidase Activity Assay Kit (Sigma-Aldrich, https://www.sigmaaldrich.com). One unit of β-glucosidase is the amount of enzyme that catalyzes the hydrolysis of 1 μmol min^{-1} substrate at pH 7.0.

β-galactosidase activity was determined using the BetaRed™ β-Galactosidase Assay Kit (NOVAGEN, https://www.novogene.com). Purified β-galactosidase was used as the control (Merck, https://www.merckmillipore.com). One unit of β-galactosidase is the amount of enzyme that generates 1 μmol min^{-1} fluorescein at pH 7.0 at 37 °C.

Pepsin activity was determined using the fluorometric Pepsin/Pepsinogen Assay Kit (Abcam, https://www.abcam.com). One unit of pepsin activity is the amount of enzyme that generates 1 μmol min^{-1} unquenched 7-methoxycoumarin-4-acetate (MCA) by hydrolysis of 1 μmol peptide substrate at 37 °C and pH 2.

2.10. Statistics

Experiments were performed using biological triplicates unless stated otherwise. Data were subjected to One-way Anova analysis of variance. Mean value was analyzed with a confidence $p \leq 0.05$.

2.11. Accession numbers

RNA sequencing data have been deposited in NCBI GEO with accession number GSE102899 (https://www.ncbi.nlm.nih.gov/geo/query/acc.cgi).

3. RESULTS

3.1. Inactivation of flbA-regulated genes

Genes *abaA*, *ATCC64974_91750*, *htfA*, and *srbA* are 2–4 fold upregulated in Δ*flbA* of *A. niger*, while *aslA*, *azf1*, and *nosA* are 2–4 fold down-regulated (Krijgsheld and Wösten, 2013). NosA, AslA, and AbaA of *A. niger* show 74 %, 66 %, and 54 % identity to their bi-directional homologues of *A. nidulans,* respectively, while SrbA shows 65 % identity to its counterpart in *A. fumigatus*. HtfA of *A. niger* shares 57 % identity to FgHtf1 of *F. graminearum,* while Azf1 has an identity of 46 % with its homolog in *S. cerevisiae*. ATCC64974_91750 shares 78 % identity with AslA of *A. niger* and therefore we now call it AslB. Genes *abaA*, *aslA*, *aslB*, *azf1, htfA*, *nosA*, and *srbA* were inactivated by CRISPR-Cas9. Inactivation of the genes was confirmed by PCR and Sanger sequencing. In addition, reintroduction of the genes in the deletion strains resulted in wild-type phenotypes. For instance, sporulation and resistance to cell wall perturbing agents was similar between the reference strain and the strains in which the deleted gene was reintroduced (Supplemental Fig. 3).

3.2. Growth and sporulation

Radial growth of the knockout strains was not severely, if at all, affected when compared to the reference strain MA234.1 when grown on PDA or a defined minimal agar medium (MMA) with glucose, sucrose, xylose, sorbitol, maltose, starch, xylan or pectin as a carbon source (Fig. 1A). Yet, biomass of strains Δ*abaA,* Δ*aslA*, Δ*nosA,* and Δ*srbA* was reduced by 18.7 %-25.9 % on MMA with glucose (MMA-G) (Fig. 1B; Table 2). Timing of sporulation, conidiophore size, and density of aerial hyphae were not affected in the knock-out strains (data not shown). By contrast, all knockout strains were affected in sporulation. The Δ*aslA*, Δ*aslB,* Δ*nosA,* and Δ*srbA* strains showed the strongest effect with a reduction of conidia formation of 50.3 %-75.0 % (Fig. 1CD; Table 2).

3.3. Stress resistance

The reference and the deletion strains were exposed to the cell wall stressors sodium dodecyl sulfate (SDS) and Congo Red (CR), the endoplasmic reticulum stress inducer dithiothreitol (DTT) as well as H_2O_2 induced oxidative stress. None of the knockout strains were affected in resistance to DTT. By contrast, all knock out strains showed increased sensitivity to SDS with the exception of Δ*abaA* that was more resistant (Fig. 2A; Table 2). Strains Δ*abaA,* Δ*nosA,* and Δ*srbA* showed increased resistance to CR, while Δ*aslA* and Δ*htfA* showed higher resistance to H_2O_2. By contrast, Δ*aslB* was more sensitive to this oxidizing agent.

The effect of gene deletion on cell wall integrity was studied in more detail by assessing the expression of genes related to α-glucan (*agsA*) and chitin (*chsC*) synthesis and to chitin deposition (*gfaA*). Genes *agsA* and *gfaA* are involved in the cell wall integrity pathway of *A. niger* (Ram et al., 2004; Damveld et al., 2005), while *chsC* has a similar function in *A. nidulans* (Fujiwara et al., 2000). qPCR showed increased expression of *agsA* in Δ*aslB* and Δ*nosA* (Fig. 2B). Expression of *chsC* was higher in Δ*abaA,* while it was lower in all other knockout strains (Fig. 2C). Expression of *gfaA* was lower in Δ*abaA,* Δ*aslA*, Δ*aslB,* and Δ*htfA* (Fig. 2D). Together, knockout strains affected in cell wall integrity showed lower expression of *chsC* either or not combined with a lower expression of *gfaA*. Also, expression of *agsA* was higher in some of these strains.

3.4. Protein secretion

The reference and the Δ*abaA*, Δ*aslA*, Δ*aslB*, Δ*azf1,* Δ*htfA,* Δ*nosA,* and Δ*srbA* strains were precultured in TM-G for 16 h, which was followed by culturing for 24 h in MM with xylose as carbon source (MM-X). Strains Δ*aslA* and Δ*aslB* formed more biomass in the liquid shaken

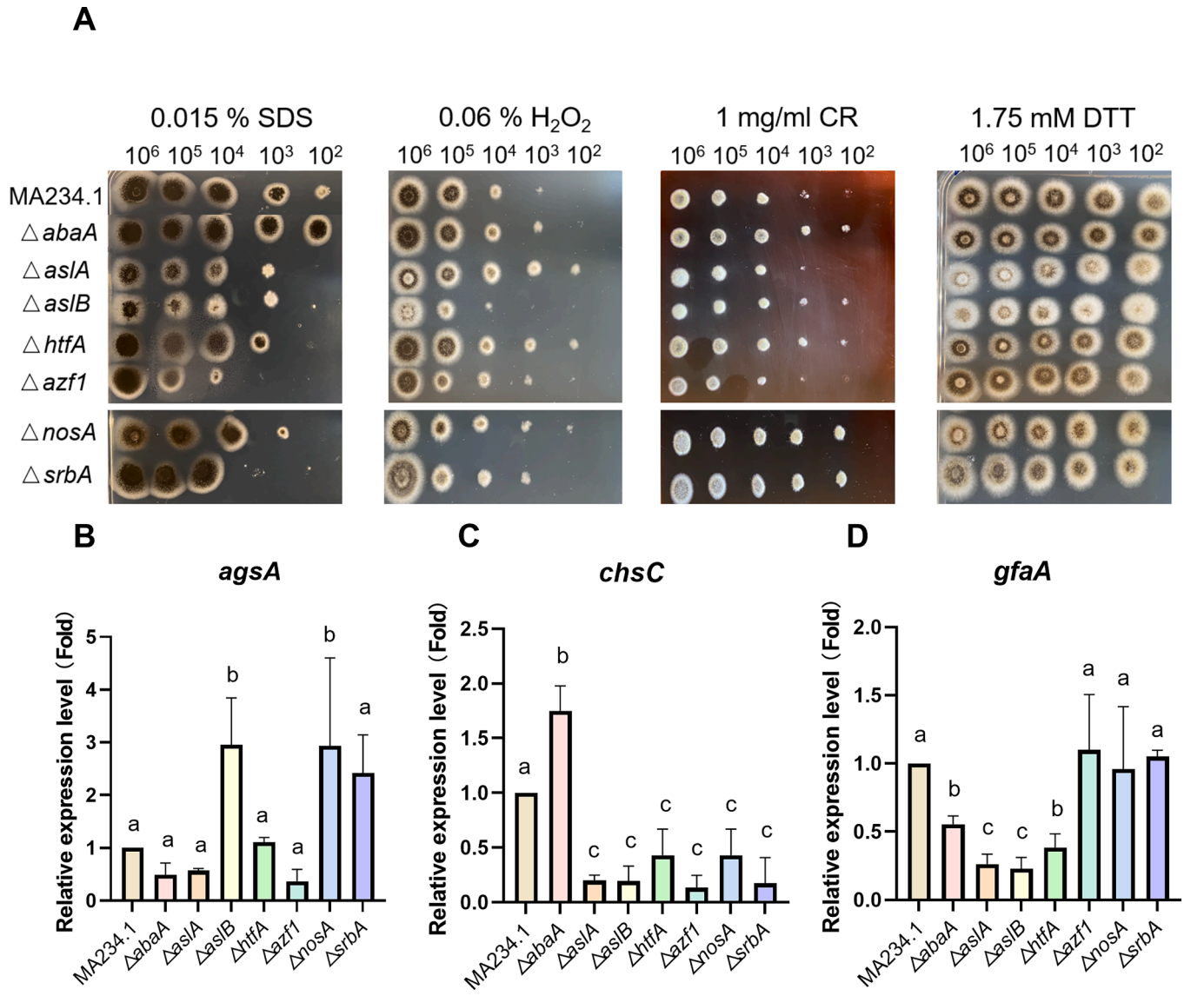

Fig. 2. Resistance of the reference and the Δ*abaA*, Δ*aslA*, Δ*aslB*, Δ*azf1*, Δ*htfA*, Δ*nosA*, and Δ*srbA* strains to 0.015 % SDS, 1.75 mM DTT, 1 mg mL^{-1} CR, and 0.06 % H_2O_2 (A) and expression of the cell wall related genes *agsA* (B), *chsC* (C), and *gfaA* (D) after 3 days of growth on MMA-G. Statistical analysis was done with One-way ANOVA with different letters indicating statistical differences between strains.

cultures (Fig. 3B; Table 2) and had the lowest pH of the culture medium (pH 5.3, 4.2, 4.3 for the reference and the Δ*aslA* and Δ*aslB* strains, respectively) (Fig. 3C; Table 2). The protein profiles after 24 h of culturing in MM-X showed increased intensity of bands at 120 kDa and 50 kDa in the case of Δ*aslA* and Δ*aslB* (Fig. 3A). Proteomics showed the presence of pepsin PepA in the 50 kDa band, while α-glucuronidase AguA, β-glucosidase BglA, and β-galactosidase LacA were identified in the 120 kDa band (Supplemental Table 2). Activity of β-glucosidase, β-galactosidase, and pepsin was determined in the culture media (there was no α-glucuronidase activity assay available). β-galactosidase activity was similar in the media of Δ*aslA* and Δ*aslB* and the reference strain (Fig. 4E). By contrast, β-glucosidase was increased 1.5-fold and 2.1-fold in Δ*aslA* and Δ*aslB*, respectively (Fig. 4D), while pepsin activity was 2.7-fold and 2.4-fold increased (Fig. 4F). Taking together, inactivation of *aslA* and *aslB* increased secretion of β-glucosidase and pepsin.

Next, β-glucosidase activity was determined after growing the reference and the Δ*aslA* and Δ*aslB* strains on processed cellulose (CM-C) (Fig. 4G). These knock out strains had a 1.6- and 1.5-fold higher β-glucosidase activity when compared to the reference strain. Co-culturing Δ*aslB* and the reference strain resulted in a β-glucosidase activity similar to that of the mono-culture of the former strain (Fig. 4G). This indicates that the β-glucosidases of the two strains have a synergistic activity (otherwise an intermediate activity would have been found). A 1.3-fold increased β-glucosidase activity was even obtained when strain Δ*aslA* was co-cultured with the reference strain compared to the Δ*aslA* culture.

Activity of amylase, xylanase, and cellulase was determined in the reference and knockout strains after growing on MM-X (Fig. 4A–C). Xylanase activity was 10.6 %-24.5 % lower in all knockout strains except for Δ*abaA* and Δ*aslA* (Fig. 4A). By contrast, amylase activity was 17.4 % and 45.2 % higher in Δ*aslA* and Δ*aslB*, respectively, while activity was 37.5 % lower in Δ*azf1* (Fig. 4B). Furthermore, strains Δ*aslA* and Δ*aslB* showed an increased cellulase activity of 19.4 % and 38.2 %, respectively (Fig. 4C).

Together, inactivation of *aslA*, *aslB*, *azf1, htfA, nosA,* and *srbA* impacts secretion of enzymes into the culture medium, which is especially the case for the former two genes.

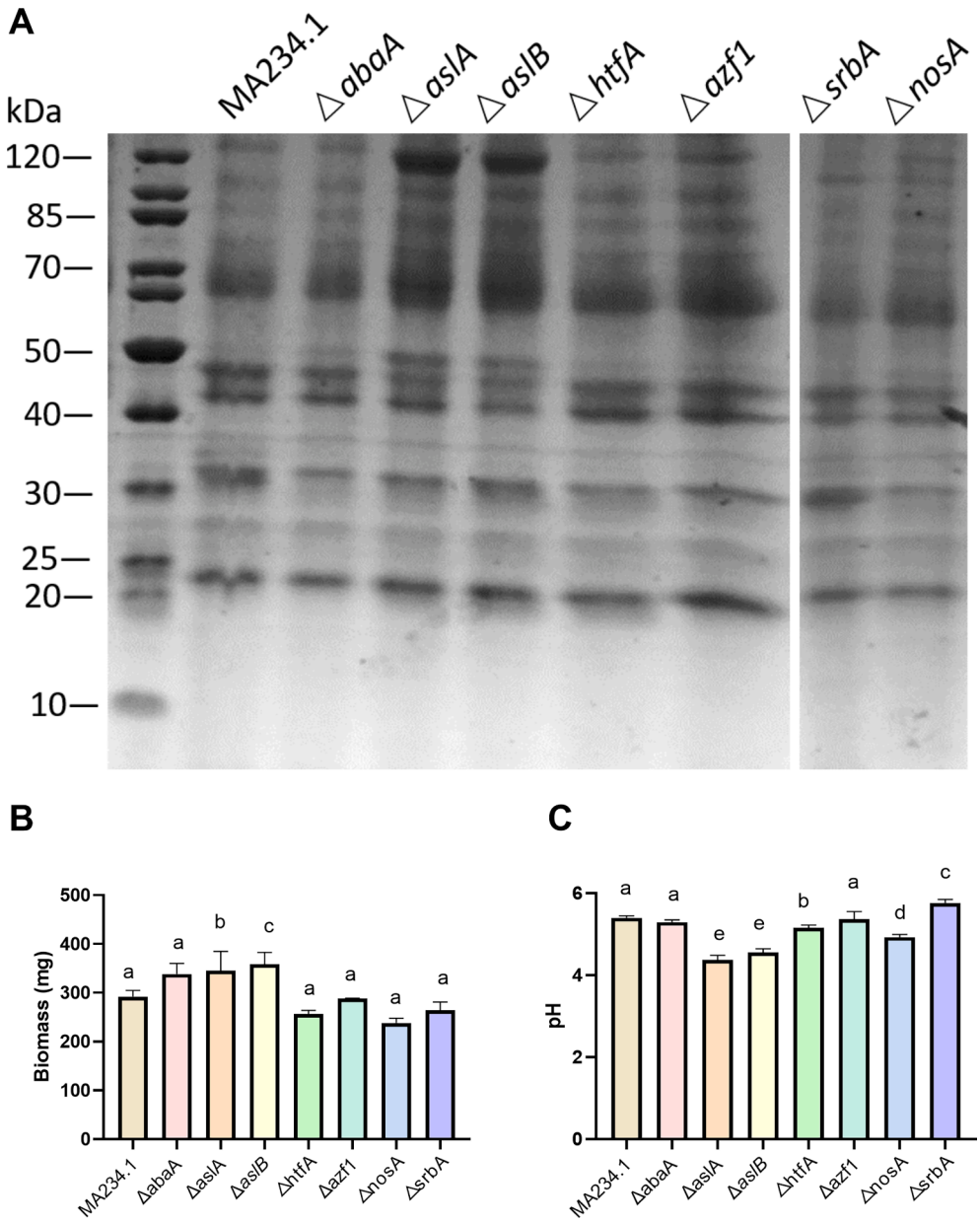

Fig. 3. Protein profiles (A), biomass (B), and pH (C) of liquid cultures of the reference and the Δ*abaA*, Δ*aslA*, Δ*aslB*, Δ*azf1*, Δ*htfA*, Δ*nosA*, and Δ*srbA* strains grown for 16 h in TM-G and 24 h in MM-X. Statistical analysis was done with One-way ANOVA with different letters indicating statistical differences between strains.

3.5. RNA profiling of liquid shaken cultures

RNA was sequenced of liquid shaken cultures of Δ*aslA*, Δ*aslB* and the reference strain that had been grown for 16 h in TM-G and for 4 h in MM-X (Supplemental Table 3). A total of 634 and 870 genes were up- and down-regulated (≥4 fold) in Δ*aslA* compared to MA234.1 (Fig. 5; Supplemental Table 4). On the other hand, 350 and 74 genes were up- and down-regulated in Δ*aslB* compared to MA234.1, respectively (Fig. 5; Supplemental Table 4). A total of 337 genes were upregulated in both Δ*aslA* and Δ*aslB*, while all 74 downregulated genes in Δ*aslB* strain were also down-regulated in Δ*aslA* (Fig. 5). A total of 2 and 377 genes were up- and down-regulated in Δ*aslA* when compared to Δ*aslB* (Supplemental Table 4).

GO analysis indicated that cellular macromolecule biosynthetic process, translation, ribosome, and structural constituent of ribosome were over-represented in the up-regulated genes of both Δ*aslA* and Δ*aslB* (Fig. 6AC). In addition, rRNA metabolic process and rRNA processing were overrepresented in Δ*aslB,* while peptide biosynthetic process was overrepresented in Δ*aslA* (Fig. 6AC). On the other hand, carbohydrate metabolic process, hydrolyzing o-glycosyl-compounds, and hydrolase activity acting on glycosyl bonds were overrepresented in the downregulated genes of Δ*aslA* and Δ*aslB* (Fig. 6BD), while this was also the case for oxidoreductase activity and hydrolase activity in Δ*aslA* (Fig. 6B).

3.6. Differentially expressed TF genes

A total of 4 and 0 TF genes were up- and down-regulated in Δ*aslB* when compared to MA234.1 (Supplemental Table 5). These four upregulated TF genes are not part of the 36 differentially expressed TF genes in Δ*flbA*. On the other hand, a total of 8 and 52 TF genes were up- and down-regulated in Δ*aslA* when compared to MA234.1 (Supplemental Table 5). Among the 36 differentially expressed TF genes in Δ*flbA* (Krijgsheld and Wösten, 2013; Aerts, 2018), five (*azf1, nosA, xlnR, prtT*, and *ATCC64974_48430*) were down-regulated in Δ*aslA* as well (Fig. 7B, Supplemental Table 6). By contrast, *aslB* and *flbD* were upregulated in

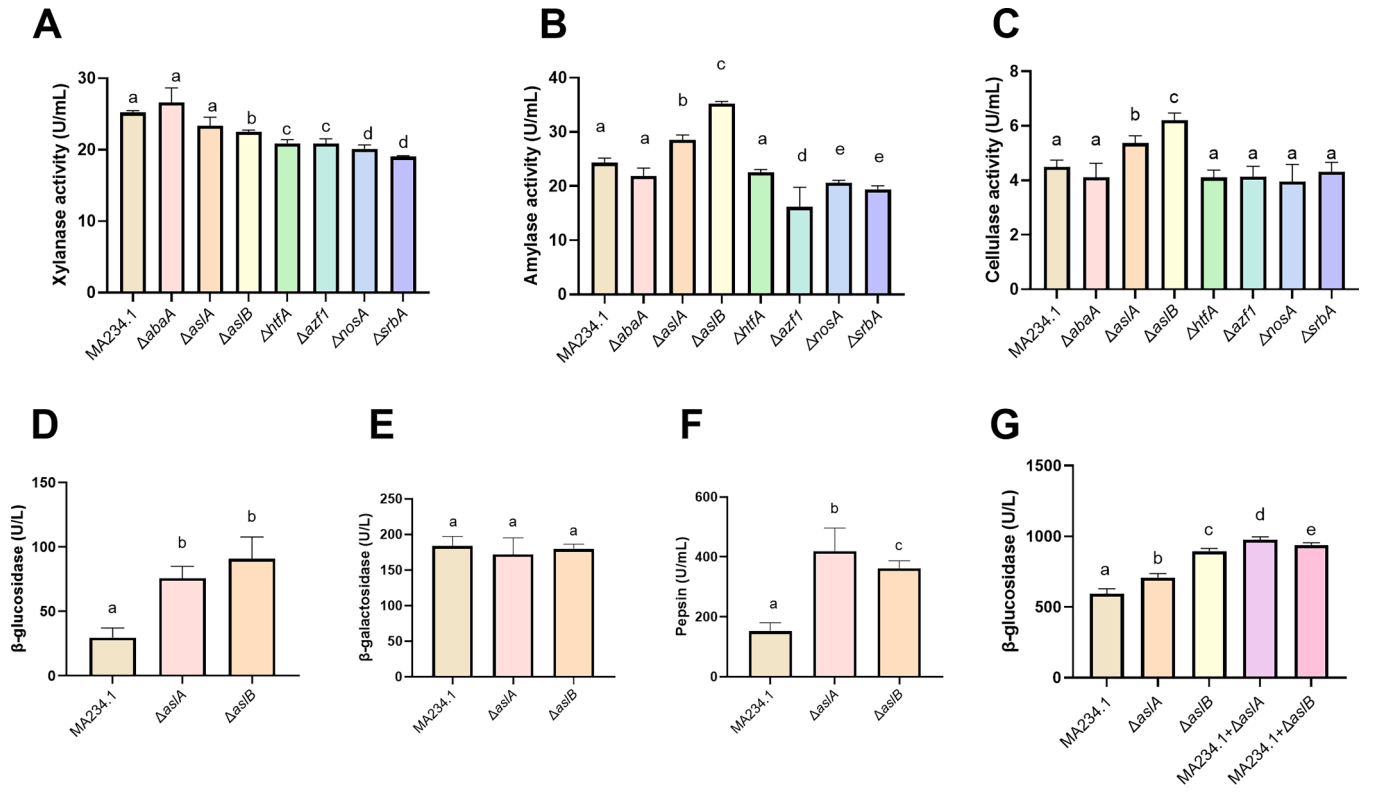

Fig. 4. Xylanase (A), amylase (B), and cellulase (C) activity in the culture medium of the reference and the Δ*abaA*, Δ*aslA*, Δ*aslB*, Δ*azf1*, Δ*htfA*, Δ*nosA*, and Δ*srbA* strains, as well as β-glucosidase (D,G), β-galactosidase (E), and pepsin (F) activity in the reference and the Δ*aslA* and Δ*aslB* strains. Cultures were grown in MM-X (A-F) and CM-C (G). Statistical analysis was done with One-way ANOVA with different letters indicating statistical differences between strains.

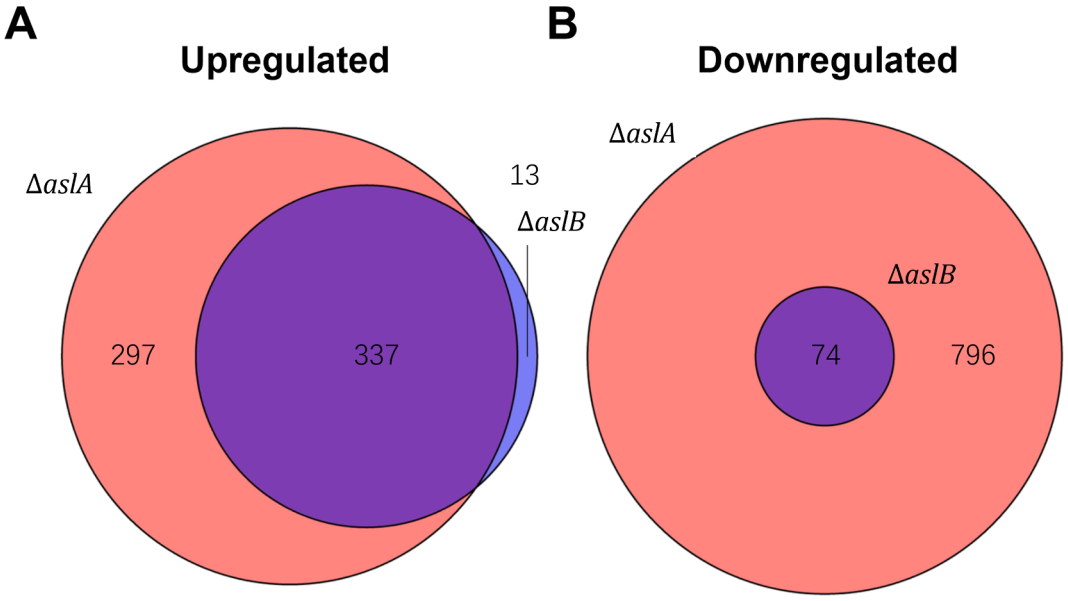

Fig. 5. Ven diagrams (A, B) showing up- and down-regulated genes in liquid shaken MM-X cultures of Δ*aslA* and Δ*aslB* when compared to MA234.1.

Δ*flbA* but downregulated in Δ*aslA,* while *abaA* was upregulated both in Δ*flbA* and Δ*aslA*. The expression level of *amyR* did neither change in Δ*flbA* (Krijgsheld and Wösten, 2013) nor did it change in Δ*aslA* and Δ*aslB*.

3.7. Differentially expressed genes related to asexual development and cell wall synthesis

A total of six out of 39 *A. niger* genes implicated in asexual reproduction (Pel et al., 2007) were differentially expressed (≥4 fold) in Δ*aslA* compared to the reference strain (Table 3; Supplemental Table 7). Three (*abaA*, *flbC,* and *flbD*) out of the six genes encode TFs, while the other three genes (*fluG, ppoA*, and *ppoC*) are involved in extracellular

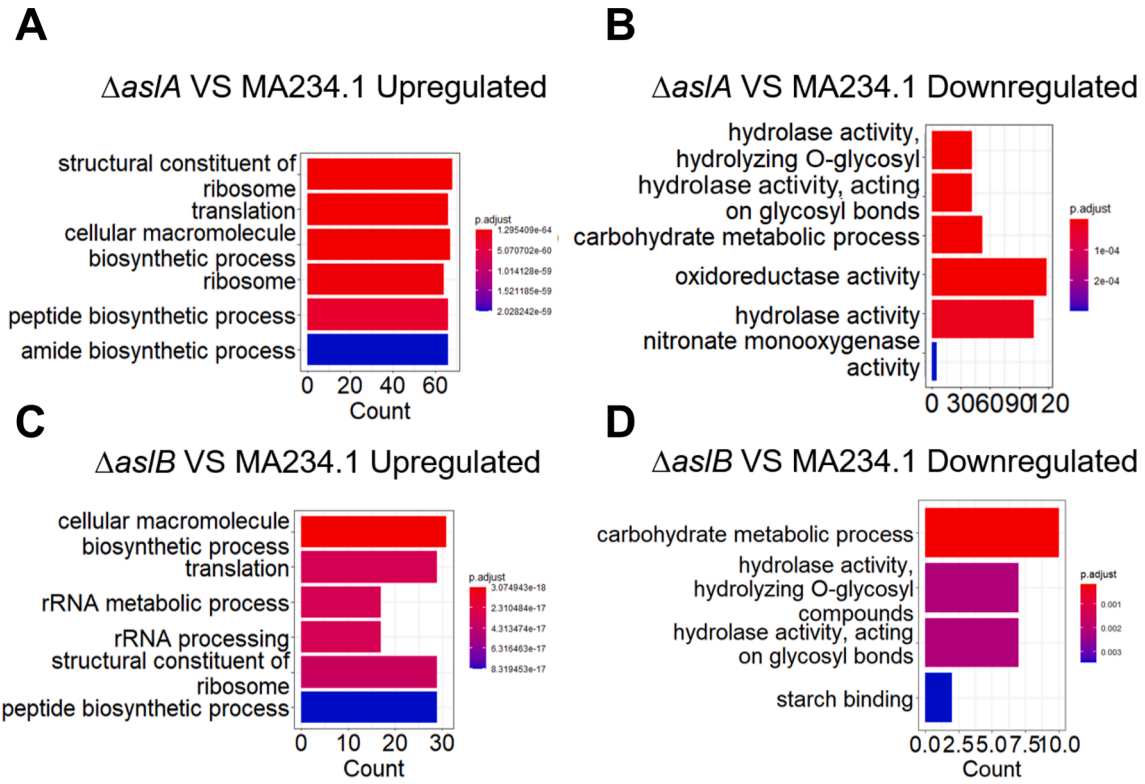

Fig. 6. GO analysis of over- (A, C) and under- (B, D) represented (≥4 fold) gene families in differentially expressed genes of Δ*aslA* (A, B) and Δ*aslB* (C, D) when compared to MA234.1.

signaling. Genes *fluG* and *abaA* were up-regulated in Δ*aslA* while *flbC*, *flbD*, *ppoA*, *ppoC* were downregulated. Surprisingly, none of the genes involved in asexual development were differentially expressed in Δ*aslB,* while *ppoC* was down-regulated in Δ*aslA* compared to Δ*aslB*.

A total of three out of 123 genes involved in cell wall synthesis (Pel et al., 2007) were up-regulated in Δ*aslA* compared to MA234.1 (i.e. glucanosyltransferase gene *gelF*, glucanase gene *agnC*, and chitin synthase gene *chsE* (Table 4; Supplemental Table 8). On the other hand, one out of the 123 genes were down-regulated in Δ*aslA* compared to MA234.1 (i.e. GPI-anchored endomannanase gene *dfgD*). Reversely, *agnC* and *agnD* were up-regulated in Δ*aslB* compared to MA234.1, the latter also being up-regulated in Δ*aslB* compared to Δ*aslA*.

3.8. Differentially expressed genes encoding proteins with a signal sequence for secretion

Out of the 634 and 350 upregulated genes in Δ*aslA* and Δ*asl*B, only 14 and 7 genes have a predicted signal sequence. These 21 genes did not include cellulase and amylase genes (Supplemental Table 9). Out of the 871 and 74 down-regulated genes in Δ*aslA* and Δ*aslB*, 112 and 18 genes have a predicted signal sequence for secretion including xylanolytic genes (Supplemental Table 9). The α-galactosidase genes *aglA* (*ATCC64974_1620*) and *aglB* (*ATCC64974_53780*) and the xylanase genes *axlA* (*ATCC64974_10330*) and *xlnD* (*ATCC64974_15350*) were down-regulated in Δ*aslA*, while the xylanase gene *bxlA* (*ATCC64974_96470*) was down-regulated in both Δ*aslA* and Δ*aslB*.

Cultures were grown on MM with xylose as carbon source. Xylose activates XlnR, which regulates xylanolytic and cellulolytic genes (van Peij et al., 1998a; van Peij et al., 1998b; Gielkens et al., 1999; de Vries and Visser, 1999; de Vries and Visser, 2001; Hasper et al., 2000; Hasper et al., 2004; de Souza et al., 2013). A total of 38 genes have been found to be regulated by XlnR (de Souza et al., 2013), of which 1 and 14 were ≥4-fold up- and down-regulated, respectively, in Δ*aslA* compared to MA234.1 (Table 5; Supplemental Table 10). The β-galactosidase gene *lacB* was upregulated, while expression of the β-galactosidase gene *lacA*, the β-glucosidase gene *bglA*, and the α-L-arabinofuranosidase genes *abfA* and *abfB* was >64-fold lower in Δ*aslA* compared to MA234.1. A total of three and one out of the 38 XlnR regulated genes were down- and up-regulated in Δ*aslB* when compared to MA234.1. Genes *lacA, abfC,* and *bxlA* were over 8-fold down-regulated, while *lacB* was over 8-fold up-regulated.

qPCR was used to quantify expression of the α-glucuronidase gene *aguA*, the β-galactosidase gene *lacA,* the β-glucosidase gene *bglA,* the cellulase gene *eglA* and the α-amylase gene *amyA*. The former gene was upregulated in Δ*aslA* and Δ*aslB* after growth for 16 h in TM-G and 4 h in MM-X, while the other genes were down-regulated or there was no effect on expression (Supplemental Fig. 4A). These findings are in line with the RNAseq data ((Supplemental Fig. 4B). By contrast, all genes were overexpressed in Δ*aslA* and Δ*aslB* compared to the reference strain after growth for 16 h on TM-G and 24 h on MM-X. This suggests an increase in cellulase, β-galactosidase, and β-glucosidase activity during late stages of culturing.

4. Discussion

Inactivation of *flbA* impacts expression of 36 TFs (Krijgsheld and Wösten, 2013; Aerts, 2018). Previously, ten of these genes have been inactivated (van den Hombergh et al., 1996; Punt et al., 2008; Meijer et al., 2009; Raulo et al., 2016; Aerts, 2018; Aerts et al., 2018; 2019; Chen et al., 2024), of which *An14g06250* does not have an apparent phenotype (Aerts, 2018). Gene *pacC* of *A. niger* (van den Hombergh et al., 1996) activates alkaline genes and represses acidic genes (Andersen et al., 2009), *prtT* is a regulator of genes encoding proteases (Punt et al., 2008), while *clrB* (Raulo et al., 2016) and *acuB* (Meijer et al., 2009) regulate genes involved in wheat straw degradation and organic acid consumption and production, respectively (Fig. 7A). Gene *flbD* is involved in conidia formation, zonal release of amylase and cellulase activity, and in resistance to the cell wall stress agent Congo Red (Chen

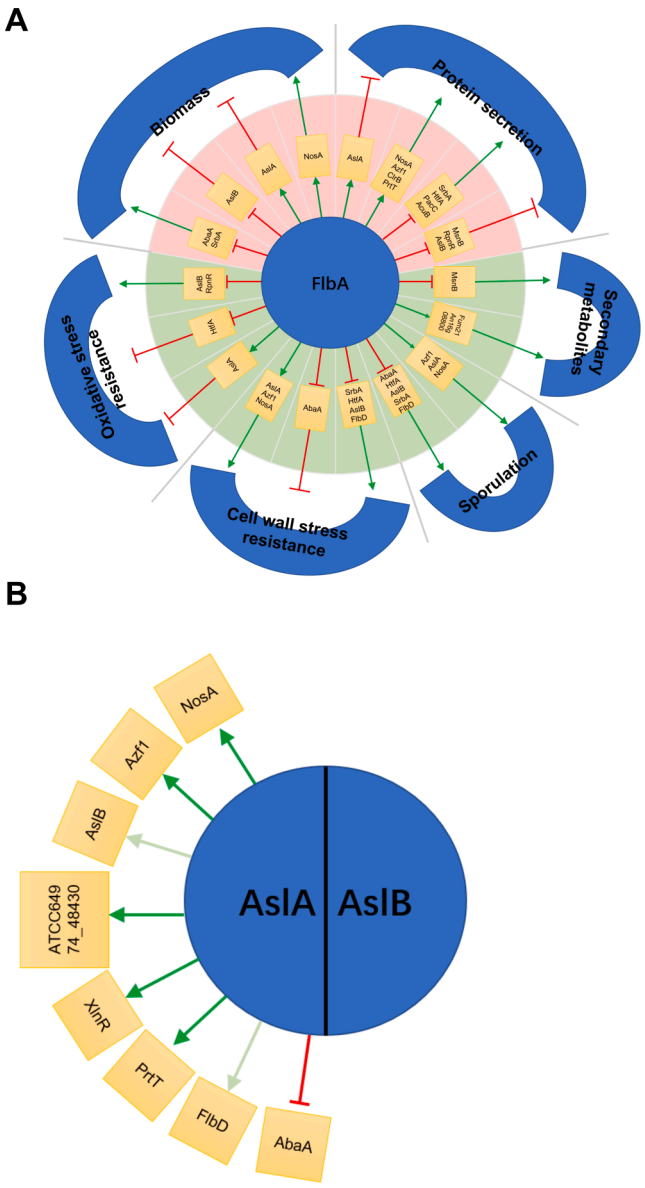

Fig. 7. Functional model of 15 out of the 36 TF genes that are differentially expressed in ΔflbA (A) and impact of inactivation of aslA and aslB on 8 out of the 36 TF genes that are differentially expressed in ΔflbA (B). An14g06250 and acuB are not part of the model. An14g06250 does not have an apparent phenotype (Aerts, 2018), while acuB regulates genes involved organic acid consumption and production (Meijer et al., 2009). Green and red shaded areas in (A) are functions that are stimulated and inhibited, respectively, by FlbA, while this is not known for functions that are not shaded. Solid cultures were used to measure the impact on biomass, oxidative stress resistance, cell wall resistance, sporulation and secondary metabolites, while liquid shaken cultures were used for protein secretion. Note that inactivation of flbD results in both increased and reduced extracellular enzyme activities in static liquid cultures (Chen et al., 2024). In (B) 5 TF genes are indicated that are downregulated (in dark green) in both ΔflbA and ΔaslA, 2 TF genes that are downregulated in ΔaslA but upregulated in ΔflbA (in light green), and one TF gene that is upregulated in both ΔflbA and ΔaslA (in red).

et al., 2024). Inactivation of *rpnR* reduces resistance to H_2O_2 and DTT and expression of ribosomal subunits and, probably as a consequence, protein secretion into the medium (Aerts et al., 2019). Instead, inactivation of *msnB* results in increased protein secretion and impacts expression of genes involved in secondary metabolites (Aerts, 2018). Genes *An16g08800* (Aerts, 2018) and *fum21* (Aerts et al., 2018) are also involved in the production of secondary metabolites. Here, an additional seven genes were inactivated that are differentially expressed in Δ*flbA*. Inactivation of these genes (i.e. *abaA, aslA, aslB, azf1, htfA, nosA*, and *srbA*) reduced production of conidia and, with the exception of *abaA,* impacted protein secretion and cell wall integrity. Furthermore, inactivation of *aslA* and *htfA* resulted in increased resistance to H_2O_2, while inactivation of *aslB* reduced resistance to this reactive oxygen species. Biomass on plates was lower in the case of Δ*abaA,* Δ*aslA*, Δ*nosA,* and Δ*srbA* and higher in liquid shaken cultures of Δ*aslA* and Δ*aslB*. Together, results imply that the pleiotropic phenotype of the Δ*flbA* strain can be explained, at least in part, by the activity of *abaA, aslA, aslB, azf1, htfA, nosA*, and *srbA*.

Genes *azf1* and *htfA* have not yet been characterized in *Aspergillus*. Here it was shown that inactivation of these genes impacted sporulation, secretion of enzymes, and cell wall integrity (Fig. 7A). Inactivation of *azf1* and *htfA* reduced xylanase activity in the culture medium, while it also reduced amylase activity in the case of *azf1*. Inactivation of either gene was accompanied by reduced expression of the chitin synthase gene *chsC,* while strain Δ*htfA* also showed reduced expression of the chitin deposition gene *gfaA*. These changes in expression may, at least in part, explain the impact of inactivation of *azf1* and *htfA* on cell wall integrity. Inactivation of *htfA* was also shown to increase resistance to H_2O_2. The phenotypes of Δ*azf1* and Δ*htfA* of *A. niger* are in line with the role of their counterparts in other fungi. Azf1 of *S. cerevisiae* is involved in cell wall maintenance when this fungus grows on a non-fermentable medium (Slattery et al., 2006), while Azf1 of *T. reesei* modulates expression of cellulase genes (Antonieto et al., 2019). The Htf1 homologue FgHTF1 of *F. graminearum* is involved in the formation of aerial hyphae and conidiophores and may also impact oxidative stress tolerance and cell wall modification (Fan et al., 2020).

Inactivation of *nosA* and *srbA* in *A. niger* impacted biomass formation on plates. Moreover, like *htfA* and *azf1*, inactivation of *nosA* and *srbA* impacted sporulation, secretion of xylanase (and amylase as well), and cell wall integrity. In fact, *nosA* and *srbA* were among the four genes with the strongest effect on sporulation. Their inactivation resulted in a reduction of 72.3 % and 50.3 % of spores. On the other hand, while Δ*azf1* and Δ*htfA* were more sensitive to SDS and CR and only SDS, respectively, Δ*nosA* and Δ*srbA* were less resistant to SDS but showed increased resistance to CR. Reduced expression of *chsC* was found in Δ*nosA* and Δ*srbA,* while *agsA* was higher expressed in the Δ*nosA* strain. These changes in expression may explain, at least in part, the cell wall integrity phenotypes of the Δ*nosA* and Δ*srbA* strains. Clearly, we studied different functions of *srbA* when compared to previous studies in *A. fumigatus* and *A. nidulans* (Chung et al., 2014, Shukla et al., 2017; Rajasenan et al., 2022; Zhang et al., 2021) and it is therefore not possible to compare the functions of this gene in different aspergilli. On the other hand, inactivation of *nosA* of *A. niger* (this study) and *A. fumigatus* (Soukup et al., 2012) reduces conidia formation and impacts growth. Yet, while inactivation of *nosA* of *A. fumigatus* increases radial growth, inactivation of *nosA* of *A. niger* reduces biomass formation.

Inactivation of *abaA* results in abnormal phialide formation and abolished sporulation in *A. nidulans* (Boylan et al., 1987; Andrianopoulos and Timberlake, 1994; Sewall et al., 1990). By contrast, Δ*abaA* of *A. niger* only showed a reduction in conidia formation. However, it also showed a reduction of biomass formation on solid medium and an increased resistance to the cell wall perturbants SDS and CR. The latter was accompanied by reduced expression of the chitin deposition gene *gfaA* and an increased expression of the chitin synthase gene *chsC*. By contrast, expression of *chsC* is reduced in strain Δ*abaA* of *A. nidulans* (Park et al., 2003). Results imply that AbaA in *A. niger*, but not *A. nidulans,* reduces the capacity to maintain cell wall integrity in wild-type strains. Moreover, results indicate that AbaA of *A. niger* is involved in sporulation and biomass formation (Fig. 7A).

Inactivation of *aslA* and *aslB* of *A. niger* reduced sporulation and impacted biomass formation, cell wall integrity, and protein secretion (Fig. 7A). Biomass formation on plate was reduced in Δ*aslA* but was increased in liquid shaken cultures of Δ*aslA* and Δ*aslB*. On the other

Table 3
Differentially expressed (≥4-fold) asexual development related genes in Δ*aslA*, Δ*aslB,* and MA234.1. Expression is expressed as normalized for gene length to fragments per kilobase per million (FPKM).

Genes	expression in Δ*aslA*	expression in Δ*aslB*	expression in MA234.1	differentially expressed in Δ*aslA* compared to MA234.1	differentially expressed in Δ*aslB* compared to MA234.1	differentially expressed in Δ*aslA* compared to Δ*aslB*
fluG	170.24	106.76	31.95	up	no	no
flbC	8.76	28	51.03	down	no	no
flbD	7.66	21.05	46.26	down	no	no
ppoA	2.31	11.59	27.87	down	no	no
abaA	10.19	4.77	0.81	up	no	no
ppoC	2.33	22.37	35.53	down	no	down

Table 4
Differentially expressed (≥4-fold) cell wall synthesis related genes in Δ*aslA*, Δ*aslB,* and MA234.1. Expression is expressed as normalized for gene length to fragments per kilobase per million (FPKM).

Genes	expression in Δ*aslA*	expression in Δ*aslB*	expression in MA234.1	differentially expressed in Δ*aslA* compared to MA234.1	differentially expressed in Δ*aslB* compared to MA234.1	differentially expressed in Δ*aslA* compared to Δ*aslB*
gelF	28.83	9.31	1.75	up	no	no
agnC	4345.60	3024.15	545.50	up	up	no
chsE	85.54	49.34	19.16	up	no	no
dfgD	0.81	5.03	13.02	down	no	no
agnD	3.45	34.26	7.69	no	up	down

Table 5
Differentially expressed (≥4-fold) XlnR regulated genes in Δ*aslA*, Δ*aslB*, and MA234.1. Expression is expressed as normalized for gene length to fragments per kilobase per million (FPKM).

Genes	expression in Δ*aslA*	expression in Δ*aslB*	expression in MA234.1	differentially expressed in Δ*aslA* compared to MA234.1	differentially expressed in Δ*aslB* compared to MA234.1	differentially expressed in Δ*aslA* compared to Δ*aslB*
aglA	4.30	8.65	27.09	down	no	no
aglB	4.43	33.83	108.91	down	no	down
lacA	0.64	88.76	419.81	down	down	down
lacB	49.00	32.84	3.83	up	up	no
bglB	2.29	10.09	41.86	down	no	no
bglC	3.71	15.18	38.17	down	no	no
bglA	32.18	832.86	2481.91	down	no	down
xlnD	1.44	6.28	23.99	down	no	no
axlA	15.01	53.22	99.00	down	no	no
abfC	2.62	35.78	187.74	down	down	down
abfA	2.02	112.81	327.74	down	no	down
abfB	0.70	317.39	1198.36	down	no	down
aglA	4.30	8.65	27.09	down	no	no
bxlA	2.21	11.81	57.08	down	down	no
eglA	7.02	23.01	62.94	down	no	no

hand, inactivation of *aslA* and *aslB* reduced resistance to SDS, but there was no effect of CR. Higher sensitivity to SDS correlated with reduced expression of *chsC* and *gfaA* in both Δ*aslA* and Δ*aslB,* while *agsA* was higher expressed in the latter strain. RNA-sequencing did not confirm these qPCR results. This may be due to the fact that mycelium from static solid cultures was used for qPCR, while mycelium of liquid shaking cultures was used for RNA sequencing. Under the latter conditions, RNA sequencing showed that Δ*aslA* over-expressed the chitin synthesis gene *chsE*, the 1,3-beta-glucanosyltransferase gene *gelF*, and the alpha-1,3-glucanase gene *agnC*, while the *endo*-mannanase gene *dfgD* was downregulated. In contrast, Δ*aslB* overexpressed the alpha-1,3-glucanase genes *agnC* and *agnD*. These data suggest that cell wall composition of Δ*aslA* and Δ*aslB* is also impacted in liquid cultures.

The Δ*aslA* and the Δ*aslB* strains (together with Δ*nosA* and Δ*srbA*) showed the strongest reduction in sporulation with 75.0 % and 60.2 %, respectively. However, this effect was less strong when compared to *aslA* in *A. nidulans*. Only 6 out of the 39 genes implicated in asexual reproduction were differentially expressed in Δ*aslA* and none of them in Δ*aslB*. Genes *fluG* and *abaA* were > 4-fold upregulated in Δ*aslA*. In contrast, *aslA* significantly stimulates the expression level of *brlA, abaA,* and *wetA* in *A. nidulans* (Kim et al., 2017).

The reduction in sporulation in Δ*aslA* and Δ*aslB* of *A. niger* was accompanied by the strongest effect on protein secretion observed in the seven knockout strains. A total of 126 and 25 genes encoding secreted proteins were differentially expressed in Δ*aslA* and Δ*aslB*. Xylanase activity was 7.2 % lower in Δ*aslB* but was not affected in Δ*aslA*. Notably, the regulatory gene of xylanolytic and cellulolytic genes, *xlnR,* was downregulated in Δ*aslA,* which was accompanied by a > 64-fold downregulation of four of its target genes. In contrast, *xlnR* was not differentially expressed in Δ*aslB*, but 4 *xlnR* regulated genes were differentially expressed in this strain.

At the protein level, β-galactosidase activity was not affected in the culture media of Δ*aslA* of Δ*aslB*, but β-glucosidase activity (*bglA*) was increased 1.5-fold and 2.1-fold in Δ*aslA* and Δ*aslB*, respectively, while pepsin activity was 2.7-fold and 2.4-fold higher. Yet, the β-galactosidase and β-glucosidase genes *bglA* and *lacA* were downregulated in the deletion strains after a 16 h incubation in TM-G followed by a 4 h incubation in MM-X. Since enzyme activity was determined later in growth (16 h TM-G + 24 h MM-X), we performed qPCR both after a total growth period of 20 h and 40 h. Overexpression of β-galactosidase and β-glucosidase related genes was observed after 40 h of culturing, but not after 20 h, in the case of Δ*aslA* and Δ*aslB*. Thus, these expression data are in agreement with the protein activity assays. Also, amylase and cellulase activity were 17.4 % and 45.2 % higher and 19.4 % and 38.2 %

higher, respectively, in Δ*aslA* and Δ*aslB* compared to the reference strain. Cellulase (*eglA*) and amylase (*amyA*) encoded genes were downregulated after 20 h of growth but over-expressed after 40 h of culturing of Δ*aslA* and Δ*aslB*. Thus, also in this case, these expression data are in agreement with the protein activity assays. Co-culturing the reference strain with either Δ*aslA* and Δ*aslB* showed that the β-glucosidase of the knockout strains had a synergistic effect with that of the reference strain, especially in the case of Δ*aslA*. Synergistic β-glucosidase activities were recently observed even within a strain by co-culturing large and small micro-colonies (Lyu et al., 2023). Future studies should therefore reveal whether the size of the micro-colonies of the reference strain and the Δ*aslA* and Δ*aslB* strains can explain the complementary cellulase activity.

The Δ*aslA* and Δ*aslB* strains are notable examples of the phenomenon of sporulation inhibited protein secretion (Levin et al., 2007; Krijgsheld et al., 2013b). This study also strengthens previous evidence that the sporulation pathway of *A. niger* is not identical to that of other aspergilli such as *A. nidulans*. Genes *fluG* (Wang et al., 2015) as well as *abaA*, *htfA* and *azf1* have the most different sporulation phenotype when compared to their counterparts in *A. nidulans*. The role of FluG in *A. niger* is most distinct. While sporulation is abolished in a *fluG* mutant of *A. nidulans,* it only represses secretion in *A. niger* (Wang et al., 2015).

Funding

This work was supported by the China Scholarship Council CSC to Xiaoyi Chen and by Consejo Nacional de Ciencia y Tecnología CONACYT to Juan P. Moran Torres.

CRediT authorship contribution statement

Xiaoyi Chen: Writing – original draft, Visualization, Validation, Methodology, Investigation, Formal analysis, Conceptualization. **Juan P. Moran Torres:** Writing – review & editing, Methodology, Investigation. **Peter Jan Vonk:** Writing – review & editing, Methodology, Investigation, Data curation. **J. Mirjam A. Damen:** Writing – review & editing, Methodology, Investigation. **Karli R. Reiding:** Writing – review & editing, Supervision. **Jan Dijksterhuis:** Investigation, Writing – review & editing. **Luis G. Lugones:** Writing – review & editing, Supervision. **Han A.B. Wösten:** Writing – review & editing, Writing – original draft, Supervision, Conceptualization.

Declaration of competing interest

The authors declare that they have no known competing financial interests or personal relationships that could have appeared to influence the work reported in this paper.

Data availability

Data have been uploaded in the GEO database

Appendix A. Supplementary material

Supplementary data to this article can be found online at https://doi.org/10.1016/j.fgb.2024.103894.

References

Aerts, D., 2018. Regulators Controlled by the Sporulation Gene *flbA* of *Aspergillus niger*. Utrecht University. PhD Thesis.

Aerts, D., Hauer, E.E., Ohm, R.A., Arentshorst, M., Teertstra, W.R., Phippen, C., Ram, A. F.J., Frisvad, J.C., Wösten, H.A.B., 2018. The FlbA-regulated predicted transcription factor Fum21 of *Aspergillus niger* is involved in fumonisin production. Antonie Van Leeuwenhoek 111, 311–332. https://doi.org/10.1007/s10482-017-0952-1.

Aerts, D., van den Bergh, S.G., Post, H., Altelaar, A.F.M., Arentshorst, M., Ram, A.F.J., Ohm, R.A., Wösten, H.A.B., 2019. FlbA-regulated gene *rpnR* is involved in stress resistance and impacts protein secretion when *Aspergillus niger* is grown on xylose. Appl. Environ. Microbiol. 85, e02282-18 https://doi.org/10.1128/AEM.02282-18.

Andersen, M.R., Lehmann, L., Nielsen, J., 2009. Systemic analysis of the response of *Aspergillus niger* to ambient pH. Genome Biol. 10, R47 https://doi.org/10.1186/gb-2009-10-5-r47.

Andrianopoulos, A., Timberlake, W.E., 1994. The *Aspergillus nidulans abaA* gene encodes a transcriptional activator that acts as a genetic switch to control development. Mol. Cell Biol. 14, 2503 https://doi.org/10.1128/mcb.14.4.2503-2515.1994.

Antonieto, A.C.C., Nogueira, K.M.V., de Paula, R.G., Nora, L.C., Cassiano, M.H.A., Guazzaroni, M.E., Almeida, F., da Silva, T.A., Ries, L.N.A., de Assis, L.J., Goldman, G. H., Silva, R.N., Silva-Rocha, R., 2019. A novel Cys2His2 zinc finger homolog of AZF1 modulates holocellulase expression in *Trichoderma reesei*. mSystems 4, e00161-19. https://doi.org/10.1128/mSystems.00161-19.

Boylan, M.T., Mirabito, P.M., Willett, C.E., Zimmerman, C.R., Timberlake, W.E., 1987. Isolation and physical characterization of three essential conidiation genes from *Aspergillus nidulans*. Mol. Cell Biol. 7, 3113–3118. https://doi.org/10.1128/mcb.7.9.3113-3118.1987.

Chen, X., Moran Torres, J.P., Wösten, H.A.B., 2024. The role of the Flb protein family in the life cycle of *Aspergillus niger*. Antonie Van Leeuwenhoek 117, 58. https://doi.org/10.1007/s10482-024-01957-x.

Chung, D., Barker, B.M., Carey, C.C., Merriman, B., Werner, E.R., Lechner, B.E., Dhingra, S., Cheng, C., Xu, W., Blosser, S.J., Morohashi, K., Mazurie, A., Mitchell, T. K., Haas, H., Mitchell, A.P., Cramer, R.A., 2014. ChIP-seq and in vivo transcriptome analyses of the *Aspergillus fumigatus* SREBP SrbA reveals a new regulator of the fungal hypoxia response and virulence. PLoS Pathog. 10, e1004487 https://doi.org/10.1371/journal.ppat.1004487.

Damveld, R.A., vanKuyk, P.A., Arentshorst, M., Klis, F.M., van den Hondel, C.A., Ram, A. F.J., 2005. Expression of *agsA*, one of five 1,3-α-D-glucan synthase-encoding genes in *Aspergillus niger*, is induced in response to cell wall stress. Fungal Genet. Biol. 42, 165–177. https://doi.org/10.1016/j.fgb.2004.11.006.

de Bekker, C., Wiebenga, A., Aguilar, G., Wösten, H.A.B., 2009. An enzyme cocktail for efficient protoplast formation in *Aspergillus niger*. J. Microbiol. Methods 76, 305–306. https://doi.org/10.1016/j.mimet.2008.11.001.

de Souza, W.R., Maitan-Alfenas, G.P., de Gouvêa, P.F., Brown, N.A., Savoldi, M., Battaglia, E., Goldman, M.H., de Vries, R.P., Goldman, G.H., 2013. The influence of *Aspergillus niger* transcription factors AraR and XlnR in the gene expression during growth in D-xylose, L-arabinose and steam-exploded sugarcane bagasse. Fungal Genet. Biol. 60, 29–45. https://doi.org/10.1016/j.fgb.2013.07.007.

de Vries, R.P., Visser, J., 1999. Regulation of the feruloyl esterase (faeA) gene from *Aspergillus niger*. Appl. Environ. Microbiol. 65, 5500–5503. https://doi.org/10.1128/AEM.65.12.5500-5503.1999.

de Vries, R.P., Visser, J., 2001. *Aspergillus* enzymes involved in degradation of plant cell wall polysaccharides. Microbiol. Mol. Biol. Rev. 65, 497–522. https://doi.org/10.1128/MMBR.65.4.497-522.

Fan, G., Zheng, H., Zhang, K., Devi, G., Opiyo, S.O., Liu, D., Li, M., Li, G., Mitchell, T.K., Yun, Y., Wang, Z., Lu, G.D., 2020. FgHtf1 regulates global gene expression towards aerial mycelium and conidiophore formation in the cereal fungal pathogen *Fusarium graminearum*. Appl. Environ. Microbiol. 86, e03024-19 https://doi.org/10.1128/AEM.03024-19.

Fujiwara, M., Ichinomiya, M., Motoyama, T., Horiuchi, H., Ohta, A., Takagi, M., 2000. Evidence that the *Aspergillus nidulans* class I and class II chitin synthase genes, *chsC* and *chsA*, share critical roles in hyphal wall integrity and conidiophore development. J. Biochem. 127, 359–366. https://doi.org/10.1093/oxfordjournals.jbchem.a022616.

Gielkens, M.M., Dekkers, E., Visser, J., de Graaff, L.H., 1999. Two cellobiohydrolase-encoding genes from *Aspergillus niger* require D-xylose and the xylanolytic transcriptional activator XlnR for their expression. Appl. Environ. Microbiol. 65, 4340–4345. https://doi.org/10.1128/AEM.65.10.4340-4345.

Hasper, A.A., Visser, J., de Graaff, L.H., 2000. The *Aspergillus niger* transcriptional activator XlnR, which is involved in the degradation of the polysaccharides xylan and cellulose, also regulates D-xylose reductase gene expression. Mol. Microbiol. 36, 193–200. https://doi.org/10.1046/j.1365-2958.2000.01843.x.

Hasper, A.A., Trindade, L.M., van der Veen, D., van Ooyen, A.J., de Graaff, L.H., 2004. Functional analysis of the transcriptional activator XlnR from *Aspergillus niger*. Microbiology 150, 1367–1375. https://doi.org/10.1099/mic.0.26557-0.

Kim, D., Paggi, J.M., Park, C., Bennett, C., Salzberg, S.L., 2019. Graph-based genome alignment and genotyping with HISAT2 and HISAT-genotype. Nat. Biotechnol. 37, 907–915. https://doi.org/10.1038/s41587-019-0201-4.

Kim, Y.J., Yu, Y.M., Maeng, P.J., 2017. Differential control of asexual development and sterigmatocystin biosynthesis by a novel regulator in *Aspergillus nidulans*. Sci. Rep. 7, 46340 https://doi.org/10.1038/srep46340.

Krijgsheld, P., Bleichrodt, R., van Veluw, G.J., Wang, F., Müller, W.H., Dijksterhuis, J., Wösten, H.A.B., 2013a. Development in *Aspergillus*. Stud. Mycol. 74, 1–29. https://doi.org/10.3114/sim0006.

Krijgsheld, P., Nitsche, B.M., Post, H., Levin, A.M., Müller, W.H., Heck, A.J., Ram, A.F.J., Altelaar, A.F.M., Wösten, H.A.B., 2013b. Deletion of *flbA* results in increased secretome complexity and reduced secretion heterogeneity in colonies of *Aspergillus niger*. J. Proteome Res. 12, 1808–1819. https://doi.org/10.1021/pr301154w.

Krijgsheld, P., Wösten, H.A.B., 2013. Transcriptome analysis of zones of colonies of the Δ*flbA* strain of *Aspergillus niger*. Fungal Genomics Biol. 3, 109 https://doi.org/10.4172/2165-8056.1000109.

Levin, A.M., Vries, R.P., Wösten, H.A.B., 2007. Localization of protein secretion in fungal colonies using a novel culturing technique; the ring-plate system. J. Microbiol. Methods 69, 399–401. https://doi.org/10.1016/j.mimet.2007.01.003.

Lyu, J., Tegelaar, M., Post, H., Moran Torres, J., Torchia, C., Altelaar, A.F.M., Bleichrodt, R.J., de Cock, H., Lugones, L.G., Wösten, H.A.B., 2023. Heterogeneity in

spore aggregation and germination results in different sized, cooperative microcolonies in an *Aspergillus niger* culture. mBio 14, e0087022. https://doi.org/10.1128/mbio.00870-22.

Meijer, S., de Jongh, W.A., Olsson, L., Nielsen, J., 2009. Physiological characterisation of *acuB* deletion in *Aspergillus niger*. Appl. Microbiol. Biotechnol. 84, 157–167. https://doi.org/10.1007/s00253-009-2027-3.

Nodvig, C.S., Nielsen, J.B., Kogle, M.E., Mortensen, U.H., 2015. A CRISPR-Cas9 system for genetic engineering of filamentous fungi. PLoS One 10, e0133085. https://doi.org/10.1371/journal.pone.0133085.

Park, J., Hulsman, M., Arentshorst, M., Breeman, M., Alazi, E., Lagendijk, E.L., Rocha, M. C., Malavazi, I., Nitsche, B.M., van den Hondel, C.A., Meyer, V., Ram, A.F.J., 2016. Transcriptomic and molecular genetic analysis of the cell wall salvage response of *Aspergillus niger* to the absence of galactofuranose synthesis. Cell. Microbiol. 18, 1268–1284. https://doi.org/10.1111/cmi.12624.

Park, B.C., Park, Y.H., Park, H.M., 2003. Activation of *chsC* transcription by AbaA during asexual development of *Aspergillus nidulans*. FEMS Microbiol. Lett. 220, 241–246. https://doi.org/10.1016/S0378-1097(03)00120-4.

Park, D.S., Yu, Y.M., Kim, Y.J., Maeng, P.J., 2015. Negative regulation of the vacuole-mediated resistance to K(+) stress by a novel C2H2 zinc finger transcription factor encoded by aslA in *Aspergillus nidulans*. J. Microbiol. 53, 100–110. https://doi.org/10.1007/s12275-015-4701-8.

Pel, H.J., de Winde, J.H., Arche, D.B., Dyer, P.S., Hofmann, G., Schaap, P.J., Turner, G., de Vries, R.P., Albang, R., Albermann, K., Andersen, M.R., Bendtsen, J.D., Benen, J. A., van den Berg, M., Breestraat, S., Caddick, M.X., Contreras, R., Cornell, M., Coutinho, P.M., Danchin, E.G., Debets, A.J., Dekker, P., van Dijck, P.W., van Dijk, A., Dijkhuizen, L., Driessen, A.J., d'Enfert, C., Geysens, S., Goosen, C., Groot, G.S., de Groot, P.W., Guillemette, T., Henrissat, B., Herweijer, M., van den Hombergh, J.P., van den Hondel, C.A.M.J.J., van der Heijden, R.T., van der Kaaij, R.M., Klis, F.M., Kools, H.J., Kubicek, C.P., van Kuyk, P.A., Lauber, J., Lu, X., van der Maarel, M.J., Meulenberg, R., Menke, H., Mortimer, M.A., Nielsen, J., Oliver, S.G., Olsthoorn, M., Pál, K., van Peij, N.N.M.E., Ram, A.F.J., Rinas, U., Roubos, J.A., Sagt, C.M.J., Schmoll, M., Sun, J., Ussery, D., Varga, J., Vervecken, W., van de Vondervoort, P.J., Wedler, H., Wösten, H.A.B., Zeng, A.P., van Ooyen, A.J., Visser, J., Stam, H., 2007. Genome sequencing and analysis of the versatile cell factory *Aspergillus niger* CBS 513.88. Nat. Biotechnol. 25, 221–231. https://doi.org/10.1038/nbt1282.

Punt, P.J., Schuren, F.H., Lehmbeck, J., Christensen, T., Hjort, C., van den Hondel, C.A. M.J.J., 2008. Characterization of the *Aspergillus niger* prtT, a unique regulator of extracellular protease encoding genes. Fungal Genet. Biol. 45, 1591–1599. https://doi.org/10.1016/j.fgb.2008.09.007.

Rajasenan, S., Osmani, A.H., Osmani, S.A., 2022. Modulation of sensitivity to gaseous signaling by sterol-regulatory hypoxic transcription factors in *Aspergillus nidulans* biofilm cells. Fungal Genet. Biol. 163, 103739 https://doi.org/10.1016/j.fgb.2022.103739.

Ram, A.F.J., Arentshorst, M., Damveld, R.A., vanKuyk, P.A., Klis, F.M., van den Hondel, C.A., 2004. The cell wall stress response in *Aspergillus niger* involves increased expression of the glutamine : fructose-6-phosphate amidotransferase-encoding gene (gfaA) and increased deposition of chitin in the cell wall. Microbiology 150, 3315–3326. https://doi.org/10.1099/mic.0.27249-0.

Raulo, R., Kokolski, M., Archer, D.B., 2016. The roles of the zinc finger transcription factors XlnR, ClrA and ClrB in the breakdown of lignocellulose by *Aspergillus niger*. AMB Express 6, 5. https://doi.org/10.1186/s13568-016-0177-0.

Sewall, T.C., Mims, C.W., Timberlake, W.E., 1990. *abaA* controls phialide differentiation in *Aspergillus nidulans*. Plant Cell 2, 731–739. https://doi.org/10.1105/tpc.2.8.731.

Shevchenko, A., Tomas, H., Havlis, J., Olsen, J.V., Mann, M., 2006. In-gel digestion for mass spectrometric characterization of proteins and proteomes. Nat. Protoc. 1, 2856–2860. https://doi.org/10.1038/nprot.2006.468.

Shukla, N., Osmani, A.H., Osmani, S.A., 2017. Microtubules are reversibly depolymerized in response to changing gaseous microenvironments within *Aspergillus nidulans* biofilms. Mol. Biol. Cell 28, 634–644. https://doi.org/10.1091/mbc.E16-10-0750.

Slattery, M.G., Liko, D., Heideman, W., 2006. The function and properties of the Azf1 transcriptional regulator change with growth conditions in *Saccharomyces cerevisiae*. Eukaryot. Cell 5, 313–320. https://doi.org/10.1128/EC.5.2.313-320.2006.

Soukup, A.A., Farnoodian, M., Berthier, E., Keller, N.P., 2012. NosA, a transcription factor important in *Aspergillus fumigatus* stress and developmental response, rescues the germination defect of a *laeA* deletion. Fungal Genet. Biol. 49, 857–865. https://doi.org/10.1016/j.fgb.2012.09.005.

Trapnell, C., Roberts, A., Goff, L., Pertea, G., Kim, D., Kelley, D.R., Pimentel, H., Salzberg, S.L., Rinn, J.L., Pachter, L., 2012. Differential gene and transcript expression analysis of RNA-seq experiments with TopHat and Cufflinks. Nat. Protoc. 7, 562–578. https://doi.org/10.1038/nprot.2012.016.

van den Hombergh, J.P., MacCabe, A.P., van de Vondervoort, P.J., Visser, J., 1996. Regulation of acid phosphatases in an *Aspergillus niger pacC* disruption strain. Mol. Gen. Genet. 251, 542–550. https://doi.org/10.1007/BF02173643.

van Leeuwe, T.M., Arentshorst, M., Erns, T., Alazi, E., Punt, P.J., Ram, A.F.J., 2019. Efficient marker free CRISPR/Cas9 genome editing for functional analysis of gene families in filamentous fungi. Fungal Biol. Biotechnol. 6, 13. https://doi.org/10.1186/s40694-019-0076-7.

van Peij, N.N.M.E., Gielkens, M.M.C., de Vries, R.P., Visser, J., de Graaff, L.H., 1998a. The transcriptional activator XlnR regulates both xylanolytic and endoglucanase gene expression in *Aspergillus niger*. Appl. Environ. Microbiol. 64, 3615–3619. https://doi.org/10.1128/AEM.64.10.3615-3619.

van Peij, N.N.M.E., Visser, J., de Graaff, L.H., 1998b. Isolation and analysis of *xlnR*, encoding a transcriptional activator co-ordinating xylanolytic expression in *Aspergillus niger*. Mol. Microbiol. 27, 131–142. https://doi.org/10.1046/j.1365-2958.1998.00666.x.

Vienken, K., Fischer, R., 2006. The Zn(II)2Cys6 putative transcription factor NosA controls fruiting body formation in *Aspergillus nidulans*. Mol. Microbiol. 61, 544–554. https://doi.org/10.1111/j.1365-2958.2006.05257.x.

Vishniac, W., Santer, M., 1957. The thiobacilli. Bacteriol. Rev. 21, 195–213. https://doi.org/10.1128/br.21.3.195-213.1957.

Wang, F., Krijgsheld, P., Hulsman, M., de Bekker, C., Müller, W.H., Reinders, M., de Vries, R.P., Wösten, H.A.B., 2015. FluG affects secretion in colonies of *Aspergillus niger*. Antonie Van Leeuwenhoek 107, 225–240. https://doi.org/10.1007/s10482-014-0321-2.

Wei, S., Hu, C., Zhang, Y., Lv, Y., Zhang, S., Zhai, H., Hu, Y., 2023. AnAzf1 acts as a positive regulator of ochratoxin A biosynthesis in *Aspergillus niger*. Appl. Microbiol. Biotechnol. 107, 2501–2514. https://doi.org/10.1007/s00253-023-12404-8.

Wösten, H.A.B., 2019. Filamentous fungi for the production of enzymes, chemicals and materials. Curr. Opin. Biotechnol. 59, 65–70. https://doi.org/10.1016/j.copbio.2019.02.010.

Wösten, H.A.B., Moukha, S.M., Sietsma, J.H., Wessels, J.G.H., 1991. Localization of growth and secretion of proteins in *Aspergillus niger*. J. Gen. Microbiol. 137, 2017–2023. https://doi.org/10.1099/00221287-137-8-2017.

Xiao, Z., Storms, R., Tsang, A., 2004. Microplate-based filter paper assay to measure total cellulase activity. Biotechnol. Bioeng. 88, 832–837. https://doi.org/10.1002/bit.20286.

Zhang, C., Gao, L., Ren, Y., Gu, H., Zhang, Y., Lu, L., 2021. The CCAAT-binding complex mediates azole susceptibility of *Aspergillus fumigatus* by suppressing SrbA expression and cleavage. Microbiologyopen 10, e1249. https://doi.org/10.1002/mbo3.1249.